HHS Public Access

Author manuscript

Nat Chem Biol. Author manuscript; available in PMC 2014 April 01.

Published in final edited form as:

Nat Chem Biol. 2013 October ; 9(10): 643–650. doi:10.1038/nchembio.1331.

Targeted Disruption of the EZH2/EED Complex Inhibits EZH2-dependent Cancer

Woojin Kim[1,2,3], **Gregory H. Bird**[2,3,4], **Tobias Neff**[5], **Guoji Guo**[1,2,3], **Marc A. Kerenyi**[1,2,3], **Loren D. Walensky**[1,2,3,4,*], and **Stuart H. Orkin**[1,2,3,6,*]

[1]Division of Pediatric Hematology/Oncology, Boston Children's Hospital, MA02115

[2]Harvard Medical School, Boston, MA 02115

[3]Pediatric Oncology, Dana-Farber Cancer Institute, Boston, MA 02115

[4]Linde Program in Cancer Chemical Biology, Dana-Farber Cancer Institute, Boston MA 02115

[5]Pediatric Hematology/Oncology/BMT, University of Colorado, Aurora, CO 80045

[6]Howard Hughes Medical Institute, Boston, MA 02115, USA

Abstract

Enhancer of zeste homolog2 (EZH2) is the histone lysine N-methyltransferase component of the Polycomb repressive complex 2 (PRC2), which in conjunction with embryonic ectoderm development (EED) and suppressor of zeste 12 homolog (SUZ12), regulates cell lineage determination and homeostasis. Enzymatic hyperactivity has been linked to aberrant repression of tumor suppressor genes in diverse cancers. Here, we report the development of stabilized alpha-helix of EZH2 (SAH-EZH2) peptides that selectively inhibit H3 Lys27 trimethylation by dose-responsively disrupting the EZH2/EED complex and reducing EZH2 protein levels, a mechanism distinct from that reported for small molecule EZH2 inhibitors targeting the enzyme catalytic domain. MLL-AF9 leukemia cells, which are dependent on PRC2, undergo growth arrest and monocyte/macrophage differentiation upon treatment with SAH-EZH2, consistent with observed changes in expression of PRC2-regulated, lineage-specific marker genes. Thus, by dissociating the EZH2/EED complex, we pharmacologically modulate an epigenetic "writer" and suppress PRC2-dependent cancer cell growth.

*Correspondence: stuart_orkin@dfci.harvard.edu (S.H.O.), loren_walensky@dfci.harvard.edu (L.D.W.).

Author contributions

W.K., L.W. and S.O. designed the experiments and wrote the manuscript. W.K. and G.B. synthesized the stapled peptides. T.N. generated MLL-AF9 cells and assisted W.K. with the colony forming assay and morphological studies. G.G. performed the high throughput microfluidic qPCR. M.K. assisted W.K. with the studies on HPC5, M1 and C1498 cell lines.

Competing financial Interests

L.D.W. is a scientific advisory board member and consultant for Aileron Therapeutics.

Introduction

Epigenetic regulation dictates how distinct cell types harness the genetic code to differentiate into diverse lineages and exert unique functions. Indeed, epigenetic modifications of DNA and histones by a variety of protein complexes constitute combinatorial codes of chromatin modification, amplifying the complexity of how genetically encoded information is employed. Epigenetic information is decoded by "reader" proteins that regulate the differential expression of genes during development and homeostasis in conjunction with transcription factors. Two broad classes of protein complexes, Trithorax (trxG) and Polycomb (PcG), are responsible for the deposition of histone marks that correlate with gene activation or repression[1–3]. TrxG is associated with an 'on state' of gene expression characterized by methylation of Lys4 of Histone H3 (H3K4), while PcG correlated with an 'off state' and trimethylation of Lys27 of Histone H3 (H3K27me3). In mammals, there are two distinct PcG complexes, Polycomb repressive complex 1 (PRC1) and Polycomb repressive complex 2 (PRC2). PRC2 catalyzes trimethylation of H3K27 and, at certain sites, facilitates the recruitment of PRC1 to methylated histones to repress target genes [1,2]. PRC2 is composed of three essential core components, enhancer of zeste homolog 2 (EZH2), suppressor of zeste 12 (SUZ12) and embryonic ectoderm development (EED). The conserved suppressor of variegation, enhancer of zeste, trithorax (SET) domain of EZH2 contains the active site for catalysis of H3K27 methylation[4]. EZH1, a close homologue of EZH2, contains a SET domain, forms an alternative PRC2 complex with Suz12 and EED, and also catalyzes H3K27 methylation.

In addition to the established roles of the epigenetic machinery in cell homeostasis and development, recent studies have implicated discrete protein subcomponents, such as EZH2, in the pathogenesis of diverse cancers [5–7]. EZH2 overexpression has been linked to repression of tumor suppressor genes and derepression of genes involved in metastasis [8,9]. In certain cancers, deregulation of EZH2 expression has been associated with pathologic alterations in microRNA levels [10,11]. Somatic mutations that alter the substrate specificity and functional activity of EZH2 have also been found in B cell non-Hodgkin's lymphoma [12–14]. Correspondingly, reduced expression of EZH2 by shRNA or siRNA induces proliferative arrest in cancer cell lines that overexpress EZH2 [15,16]. The genetic ablation of *Ezh2* alone prevents the development of a murine T cell lymphoma that results from inactivation of Snf5, a core component of the Swi/Snf remodeling complex [17]. Collectively, these findings implicate EZH2 deregulation in the development and maintenance of cancer, and highlight its potential as a therapeutic target.

To disable the PRC2 complex in cancer and thereby inhibit unrestrained cell proliferation, we sought to target the interaction between EZH2 and EED, which is required for enzymatic activity [18,19]. Whereas the pharmaceutical industry has focused on the development of small molecule inhibitors to block the methyltransferase active site of EZH2 [20,21], we have developed an alternative strategy that blocks both EZH1 and EZH2 activity by dismantling the PRC2 complex itself through disruption of protein interactions. The essential alpha-helical domain of EZH2 (aa 40-68) that engages EED established the basis for designing hydrocarbon-stapled derivatives to disrupt the specific protein interaction[22]. Non-natural amino acids with olefinic side chains were substituted at (i, i+4) positions within the EZH2

alpha-helical sequence, followed by ruthenium-catalyzed olefin metathesis, to yield stabilized alpha-helix of EZH2 (SAH-EZH2) peptides. Our lead, cell permeable analog effectively targeted EED *in situ*, dissociated the EZH2/EED complex, and impaired the function of PRC2, as reflected by reduction of the H3K27me3 and EZH2 protein levels, and increased expression of PRC2-regulated cell differentiation marker genes. In response to SAH-EZH2 treatment, murine MLL-AF9 leukemia cells, which are PRC2-dependent, manifested growth arrest and monocytic/macrophage differentiation, in accordance with the phenotypic consequences of shRNA-mediated reduction of EZH2 (or EED) or genetic ablation of *Ezh2* (or *Eed*) [23,24]. In evaluating SAH-EZH2 activity alongside the small molecule EZH2 inhibitor GSK126[21] in a series of B-cell lymphoma lines, we observed sequence-specific anti-proliferative responses, transcriptional modulation, cellular specificity, and a distinct mechanism of action for SAH-EZH2. Thus, we report a pharmacologic approach to epigenetic modulation, and suppression of PRC2 function, in particular, by targeted disruption of the EZH2/EED complex with a stapled peptide modeled after an essential EED-interacting domain.

Results

Synthesis and EED-Binding Activity of SAH-EZH2 Peptides

Hydrocarbon stapling has been applied to restore the natural structure of alpha-helical binding motifs, yielding bioactive agents to dissect and target intracellular protein interactions [25,26]. To disrupt the PRC2 complex, we designed stapled peptides of variable length based on the alpha-helical, EED-binding domain of EZH2 that comprises amino acids 40-68[22]. We sampled two staple positions located on the non-interacting helical surface (Fig. 1a) and measured the binding affinity of FITC-labeled SAH-EZH2 peptides for EED using fluorescence polarization (FP) (Fig. 1b, 1c) and co-immunoprecipitation (Fig. 1d) assays. Both the A and B staples enhanced alpha-helicity relative to the unmodified peptide (Supplementary Results, Supplementary Fig. 1) and the corresponding constructs showed similar activity in both *in vitro* binding assays. However, significant differences emerged upon comparison of SAH-EZH2 peptides with different length. The longest constructs, SAH-EZH2$_A$(40-68) and SAH-EZH2$_B$(40-68) displayed the most potent dose-responsive EED-binding activities, followed by SAH-EZH2$_A$(42-68) and SAH-EZH2$_B$(42-68). The foreshortened SAH-EZH2$_A$(42-64) and SAH-EZH2$_B$(42-64) peptides lacking the IQPV motif exhibited no appreciable engagement of recombinant EED by FP or of expressed HA-EED by anti-FITC pull down (Fig. 1d). These data are consistent with structure-function studies that documented the critical role of I65, P67 and V68 in the EZH2/EED interaction [22]. Thus, we identified SAH-EZH2 constructs comprising amino acids 40-68 and 42-68 as submicromolar EED binders.

In preparation for phenotypic studies in treated cells, we evaluated the cellular uptake of SAH-EZH2 peptides in MLL-AF9 leukemia cells exposed to FITC-labeled derivatives, followed by fluorescence analysis of electrophoresed cellular extracts (Fig. 1e). SAH-EZH2$_A$ peptides generally displayed enhanced cellular uptake in comparison with the corresponding constructs bearing the B-position staple, with the intermediate and shortest peptides exhibiting the most robust dose-responsive uptake. Based upon EED-binding

potency and observed cellular penetration, SAH-EZH2$_A$(42-68) emerged as the lead construct for optimization and biological testing.

Suppression of H3K27 Methylation by EZH2/EED Dissociation

We previously observed that reducing net negative charge by neutralizing negatively charged residues, such as Asp and Glu, enhances cellular uptake of stapled peptides [25,27]. Sequence comparison of EZH2 homologs indicates that Glu54 is not conserved, suggesting that this residue is dispensable for binding to EED [22]. Therefore, we mutated the non-interacting Glu54 residue of SAH-EZH2$_A$(42-68) to Gln (Fig. 1a and Fig. 2a). Indeed, we observed further enhancement of cellular uptake, as measured by fluorescence scan of FITC-SAH-treated lysates (Fig. 2b) and correlative confocal microscopy (Fig. 2c). Importantly, the Glu54Gln mutant retained comparable *in vitro* binding activity to the parental stapled peptide (Supplementary Fig. 2). To generate a negative control peptide for cellular studies, we mutated Glu59 - a highly conserved residue among EZH2 homologs - to Gln in an effort to disrupt the salt bridge between Arg200 of EED and Glu59 of EZH2 at the binding interface (Fig. 1a and Fig. 2a) [22]. We found this double mutant construct to manifest similar cellular penetration (Fig. 2b) but markedly reduced in vitro EED binding activity (Supplementary Fig. 2). Consistent with these findings, confocal microscopy documented robust cellular uptake and nuclear localization of both SAH-EZH2$_A$-E54Q and SAH-EZH2$_A$-E54Q/E59Q (hereafter referred to as SAH-EZH2and SAH-EZH2$_{MUT}$, respectively) (Supplementary Fig. 3). We next evaluated the kinetics of cellular uptake in serum-containing media and intracellular stability (Supplementary Fig. 4). Whereas the unmodified FITC-EZH2 peptide showed no detectable intracellular accumulation, both SAH-EZH2 peptides and a TAT-EZH2 construct were detectable by 1 hour. Interestingly, the time course analysis documented that both SAH-EZH2 and SAH-EZH2$_{MUT}$ peptides showed progressive accumulation and persisted in full-length form, whereas the TAT-EZH2 peptide was undetectable at 2 hours. These data indicate that hydrocarbon stapling of the EZH2 peptide sequence confers not only robust cellular uptake but also enables intracellular persistence to both SAH-EZH2 and SAH-EZH2$_{MUT}$, yet only SAH-EZH2 effectively co-precipitated native EED from MLL-AF9 cells (Supplementary Fig. 5), consistent with the differential EED binding activities of SAH-EZH2 and SAH-EZH2$_{MUT}$ (Supplementary Fig. 2)

Since the catalytic activity of PRC2 depends on the interaction between EZH2 and EED, we explored the capacity of SAH-EZH2 to disrupt EED engagement with EZH2, and its homolog EZH1. Of note, EZH1 shares 86% amino acid identity with the EED-binding domain of EZH2, and is believed to form an alternate, catalytically active PRC2 complex with EED and Suz12 [28–30]. In *Ezh2*$^{-/-}$ murine embryonic stem cells, EZH1 partially compensates for loss of EZH2 and maintains H3K27me3 at a subset of developmental genes [28]. Indeed, HA-EED co-immunoprecipitated Flag-EZH1 and Flag-EZH2 upon co-expression in sf21 cells (Supplementary Fig. 6). When incubated with these purified EZH1/EED and EZH2/EED complexes, we observed dose-responsive dissociation of the protein interactions for SAH-EZH2, but not for the mutant control (Fig. 2d). To determine if the capacity of SAH-EZH2 to target and dissociate these complexes functionally impaired PRC2 methyltransferase activity, we treated MLL-AF9 cells with SAH-EZH2 and detected

histone modification by western blot and flow cytometry. As for the small molecule EZH2 inhibitors [20,21], we employed an extended treatment course (7 days), owing to the prolonged half-life of the H3K27me3 mark.[31] Both experimental read-outs documented that SAH-EZH2 treatment decreased H3K27me3 (Fig. 2e and Supplementary Fig. 7). Inhibition of H3K27 methylation was also dose-responsive over a 1–10 μM range, with no H3K27me3 observed at 10 μM. The selectivity of SAH-EZH2 activity was highlighted by the inactivity of SAH-EZH2$_{MUT}$ and the lack of a SAH-EZH2 effect on the H3K4, H3K9 and H3K36 methyl marks (Fig. 2f). Thus, SAH-EZH2 targeted native EED, dissociated its interactions with EZH1 and EZH2, and selectively decreased trimethylation of H3K27.

SAH-EZH2 Arrests Proliferation of MLL-AF9 Leukemia Cells

Since MLL-AF9 cells are dependent on EZH2 and the PRC2 complex for growth [23,24], we explored whether the biochemical activity of SAH-EZH2 translated into an anti-proliferative effect. We treated MLL-AF9 cells for an extended incubation period and noted significantly slowed growth by eight days for SAH-EZH2- but not mutant control-exposed cells (Fig. 3a). These data are consistent with prior studies in which knockdown or knockout of EZH2 or EED impaired proliferation of MLL-AF9 cells [23,24].

To investigate the mechanism of growth arrest, we stained cells with Annexin V-PE and 7-AAD after 2, 4 and 8 day incubations with SAH-EZH2 or mutant control peptide, followed by flow cytometric analysis. No increase in apoptotic cells was observed upon treatment with SAH-EZH2 peptides for 8 days (Fig. 3b), whereas exposure to the chemotherapeutic agent, camptothecin, triggered a robust apoptotic effect. Continued monitoring for apoptotic effects through 16 days of treatment revealed only a small increase in Annexin V/7-AAD positivity above baseline for both peptides (Supplementary Fig. 8), indicative of a sequence-independent effect likely related to the prolonged treatment, which contrasted to the sequence-specific anti-proliferative effect observed throughout the treatment period (Fig. 3a). We then investigated whether the observed decreased growth of MLL-AF9 cells upon exposure to SAH-EZH2 was associated with modulation of the cell cycle using BrdU incorporation and 7-AAD staining. Whereas flow cytometric analysis of SAH-EZH2-treated MLL-AF9 cells showed no cell cycle effects at day 3 of treatment (data not shown), an increased percentage of cells in G0/G1 phase and a corresponding decrease in G2/M was observed by day 6 (Fig. 3c and Supplementary Table 1). Compared to cells treated with the mutant control stapled peptide, SAH-EZH2 led to an increase of cells in G0/G1 phase from 42.0% to 50.8%, and a decrease in G2/M phase from 6.7% to 3.2%. These data suggest that the effect of SAH-EZH2 on MLL-AF9 cell proliferation resulted from reduction of the fraction of cells in the G2/M phase. Interestingly, knockdown or genetic ablation of *Ezh2* was previously reported to derepress the cell cycle inhibitory Ink4A/Arf locus [32,33]. Consistent with this finding, SAH-EZH2 treatment of MLL-AF9 cells increased p19ARF levels, whereas cells treated with SAH-EZH2$_{MUT,}$ or no peptide, showed little to no p19ARF expression (Fig. 3d). Taken together, these data indicate that the observed proliferative arrest of cells treated with SAH-EZH2 derives from a cell cycle blockade that is associated with increased expression of p19ARF.

SAH-EZH2 Induces Differentiation of MLL-AF9 Leukemia

As MLL-AF9 cells are EZH2-dependent and manifest differentiation blockade due to epigenetic deregulation[34], we monitored the impact of SAH-EZH2-mediated disruption of PRC2 activity on the morphology of treated cells. We exposed MLL-AF9 cells to SAH-EZH2 for 14 days and then replated the cells in methylcellulose with continued compound incubation. SAH-EZH2 treatment decreased colony-forming capacity by 70% after 7 days of plating (Fig. 4a and Supplementary Fig. 9) compared to vehicle control. No effect was observed with SAH-EZH2$_{MUT}$. Whereas vehicle- and SAH-EZH2$_{MUT}$-treated cells retained the morphology of immature leukemic blasts, exposure to SAH-EZH2 triggered myeloid cell maturation, characterized by monocyte/macrophage morphology (Fig. 4b). Positive staining of SAH-EZH2-treated cells with the macrophage specific antibody F4/80 confirmed these visual findings (Fig. 4c). Whereas anti-F4/80 staining also revealed a relatively small increase in positivity for SAH-EZH2$_{MUT}$-treated cells, likely related to weak but measurable residual EED-binding activity (Supplementary Fig. 2), we observed no impact of the mutant peptide on cell morphology (Fig. 4b). The observed differentiation upon SAH-EZH2 treatment phenocopies the induced differentiation of MLL-AF9 cells upon shRNA knockdown or genetic ablation of *Ezh2* or *Eed* [23,24].

We further demonstrated the specificity of SAH-EZH2 modulation of PRC2-controlled pathways using real time qPCR analysis of transcripts representing genes of 288 cell surface markers (Fig. 4d). SAH-EZH2, but not the vehicle or SAH-EZH2$_{MUT}$ control, induced expression of discrete monocyte and macrophage lineage-specific markers, including Adam8, Fcer1a, and ACE (Fig. 4e), and suppressed other markers (for example, CD133) (Fig. 4f), which are associated with hematopoietic stem cells and populations of cancer stem cells [35–37]. Downregulation of CD133 is observed upon differentiation of monocyte/granulocyte progenitors to mature monocytes/granulocytes[38]. Moreover, highly enriched MLL-AF9 leukemic stem cells (called MLL-AF9 L-GMP) express appreciably higher levels of CD133 than more differentiated leukemic Lin$^+$/kit$^-$ blast cells harvested from mice (Supplementary Fig. 10).

Unique Mechanism of SAH-EZH2 anti-proliferative activity

To probe the selectivity of the anti-proliferative effects of SAH-EZH2, we evaluated proliferative and morphologic responses in an immortalized, but non-tumorigenic, primitive hematopoietic progenitor cell line (HPC5), and two mouse myeloid leukemia cell lines (M1 and C1492). HPC5 cells were originally derived from adult bone marrow cells immortalized by expression of the LIM homeobox gene, lhx2 [39]. These cells are unique in that they partially reconstitute hematopoiesis in lethally irradiated mice without causing leukemia. As observed for MLL-AF9 cells, SAH-EZH2, but not its mutant derivative, inhibited the proliferation of C1498 and M1 myeloid leukemia cells; the non-tumorigenic HPC5 cells showed no response (Supplementary Fig. 11). Correspondingly, the progenitor-like morphology of HPC5 cells was unaffected by treatment with vehicle, SAH-EZH2$_{MUT}$, or SAH-EZH2 (Supplementary Fig. 11), which contrasted to the striking effect of SAH-EZH2 on differentiation of MLL-AF9 cells (Supplementary Fig. 11). In addition, SAH-EZH2 had no effect on the viability of the non-leukemic transformed cell line 32D (Supplementary Fig. 12). These data are consistent with the previous observation that shRNA knockdown of

PRC2 components EED and Suz12 significantly decreased the proliferation of MLL-AF9;Nras^{G12D} cells but had minimal impact on the proliferation of the non-leukemic transformed cell line 32D [24]. Thus, we found that SAH-EZH2 treatment is selective in inducing proliferation arrest and differentiation of leukemic hematopoietic cells.

As small molecule inhibitors that target the catalytic site of EZH2 have been described recently[20,21], we tested the activity, selectivity, and mechanism of action of SAH-EZH2 alongside an exemplary molecule, GSK126. Whereas SAH-EZH2 induced dose-responsive reduction in H3K27me3 at a dose range that correspondingly impairs MLL-AF9 cell viability, GSK126 was more potent in reducing H3K27me3 across the 1–10 μM dose range (Supplementary Fig. 13), yet manifested a paradoxically weaker effect on cell viability (Fig. 5a, Supplementary Fig. 13). In the non-leukemic 32D cells, which showed no response to SAH-EZH2 treatment, GSK126 manifested a comparable degree of cytotoxicity to that observed for the small molecule in MLL-AF9 cells (Supplementary Fig. 12). In MDA-MB231 (breast cancer) and DU145 (prostate cancer) lines, which have been reported to be driven by pathologic EZH2 activity unrelated to trimethylation of H3K27[40,41], SAH-EZH2 dose-responsively impaired viability, but GSK126 had no effect (Supplementary Fig. 14). To examine potential differences in mechanism of action of SAH-EZH2 and GSK126, we assessed the effect of each treatment on the level of EZH2 protein. We reasoned that dissociation of the EZH2/EED complex by SAH-EZH2 may impair not only the enzymatic activity of EZH2 activity but also impact protein stability. Indeed, we observed that SAH-EZH2, but not GSK126, treatment led to a dose-responsive decrease in EZH2 protein levels in MLL-AF9 cells (Fig. 5b). This result highlights a distinct mechanism of action of SAH-EZH2.Differential effects on gene expression in MLL-AF9 cells were also observed for SAH-EZH2 vs. GSK126 treatments. For example, changes in Adam8, ACE and CD133 levels were more pronounced upon exposure to SAH-EZH2, whereas Fcer1a was markedly upregulated by treatment with GSK126 (Fig. 5c).

To expand the analysis to an additional cellular context, we examined the activities of SAH-EZH2 and GSK126 in a series of B-cell lymphomas. SAH-EZH2 impaired the viability of EZH2-mutant bearing Karpas422 (EZH2 Y641N) and Pfeiffer (EZH2 A677G) cells, with greater potency observed in Karpas422 than Pfeiffer (Fig. 5d and Supplementary Fig. 15). However, we observed no significant effect of SAH-EZH2 treatment on OCI-LY19 cells, which express wild-type EZH2. The distinct effects of SAH-EZH2 on cell viability were not related to differential peptide uptake, which was similar across cell lines in serum-containing media (Supplementary Fig. 16). Interestingly, the relative potency of SAH-EZH2 in Karpas422 vs. Pfeiffer cells appeared to correlate with the degree of dose-responsive decrease in EZH2 protein levels (Supplementary Fig. 17). Treatment with GSK126 also reduced the viability of Karpas422 and Pfeiffer cells, but at the highest dose level of 10 μM also impaired the viability of OCI-LY19 cells (Fig. 5d), which contrasted to the lack of activity of another EZH2 inhibitor, EPZ005687, at 10 μM in this cell line[20]. As observed for MLL-AF9 cells, both SAH-EZH2 and GSK126 reduced H3K27me3 in Karpas422 cells (Supplementary Fig. 18). Whereas GSK126 exhibited more potent inhibition of H3K27 trimethylation compared to SAH-EZH2 in Karpas422 cells in the 1–10 μM dose range (Supplementary Fig. 18), the two compounds showed similar impairment of cell viability (Fig. 5d). Importantly, the dose-responsive effect of SAH-EZH2 on cell viability in both

Karpas422 and MLL-AF9 cell lines correlated with the observed dose-responsive inhibition of H3K27 trimethylation and reduction of EZH2 protein levels over the same dose range (Fig. 5a and 5b, Supplementary Fig. 13, 17 and 18).

Given the distinct mechanisms of action of SAH-EZH2 and GSK126, we explored whether co-administration of the two compounds would enhance the anti-proliferative effects. Indeed, we found that combined treatment of MLL-AF9 and Karpas422 cells with SAH-EZH2 and GSK126 dose-responsively enhanced cellular activity compared to that of the respective compounds administered as single agents, with evidence of synergy by Calcusyn analysis (Combination indices [CI] of 0.11 and 0.74 for MLL-AF9 and Karpas 422, respectively; CI<1 reflects synergy) (Fig. 5e, Supplementary Fig. 19). Taken together, these data indicate that SAH-EZH2 manifested a unique and complementary mechanism of action by targeting EED, dissociating the EZH2/EED complex, and reducing EZH2 protein levels.

Discussion

Alterations of chromatin landscape, including DNA methylation and histone modifications, play critical roles in regulating gene expression. Interpretation of these epigenetic marks by “reader” proteins is associated with gene activation or repression, depending in part on the combination of epigenetic marks deposited by “writer” proteins. Frequent reports of genetic lesions affecting the function of “reader” and “writer” proteins in cancers have linked deregulation of these proteins to oncogenesis [42]. EZH2 is a “writer” that catalyzes methylation of histone H3K27 and has been implicated in a diversity of cancers. As such, EZH2 has emerged as a high priority target for therapeutic development [5–7,43].

DZNep has been characterized as a small molecule EZH2 inhibitor that disrupts PRC2 and manifests anti-tumor activity in a variety of cancers [44–46]. Recent evidence suggests that DZNep is a global inhibitor of histone methylation[46], consistent with its pharmacologic impairment of *S*-adenosylhomocysteine (S-AdoHcy) hydrolase activityand the synthesis of *S*-adenosylmethionine (S-AdoMet), a global methyl group donor for diverse methyltransferases[47,48]. DZNep-mediated inhibition of S-AdoMet results in global inactivation of diverse methyltransferases. Therefore, DZNep fails to act as a selective EZH2 antagonist. In contrast, the recently reported small molecules that directly inhibit the catalytic site of EZH2 demonstrate more selective effects [20,21].

Here, we report an alternative strategy for selective targeting of EZH2 methyltransferase activity by disrupting the interaction of EZH2 and EED with a hydrocarbon-stapled peptide that mimics the alpha-helical EED binding domain of EZH2. All-hydrocarbon stapling has been successfully applied to stabilize alpha-helical structures, enhance target binding affinity, and confer protease resistance and membrane penetration for a diversity of bioactive helical peptides [25,26]. We found that our lead SAH-EZH2 peptide bound directly to EED, dissociated EZH1/EED and EZH2/EED complexes, and reduced the H3K27 methyltransferase activity of the PRC2 complex. Indeed, dual targeting of PRC2-EZH1 and PRC2-EZH2 by genetic ablation of *Eed* is more effective at inhibiting the oncogenic activity of MLL-AF9 leukemia cells *in vivo* than eliminating *Ezh2* alone [23]. Correspondingly, co-expression of EZH1 and EZH2 shRNA leads to synergistic inhibition of MLL-AF9

leukemia cell proliferation, whereas shRNA knockdown of either EZH1 or EZH2 alone manifested only weak or no inhibitory effect *in vivo* [24]. Thus, pharmacologic impairment of both PRC2-EZH1 and PRC2-EZH2 is predicted to be a more effective means of silencing PRC2 than targeting EZH2 alone.

We find that the selective blockade of PRC2 methyltransferase activity by SAH-EZH2 translates into growth arrest and differentiation of MLL-AF9 cells. The functional consequences of this SAH-EZH2-induced epigenetic modulation were underscored by increased expression of macrophage-associated genes and positive staining with a macrophage-specific antibody, findings that reflect induced monocyte/macrophage differentiation of MLL AF9 cells. The anti-proliferative activity of SAH-EZH2 extended to EZH2-dependent B-cell lymphomas, in which dose-responsive and peptide sequence-dependent suppression of H3K27 trimethylation, EZH2 protein levels, and cancer cell viability was also observed. Whereas both SAH-EZH2 and the small molecule EZH2 inhibitor GSK126 reduce H3K27 trimethylation, GSK126 targets and inhibits the catalytic site of EZH2, whereas SAH-EZH2 dissociates the enzymatic complex and also decreases EZH2 protein levels. These distinct mechanisms of action may account for some of the observed differences in cellular effects and highlight the potential utility of combined treatment. Thus, SAH-EZH2-based targeting of the PRC2 complex may represent an alternative and complementary strategy for selectively arresting the proliferation of EZH2-dependent human cancers.

To our knowledge, this is the first example of a selective pharmacologic strategy for epigenetic modulation based on disruption of the intracellular binding interface between an epigenetic “writer” and its essential cofactor. Because epigenetic “writers” bind differentially to multiple cofactors and form diverse functional complexes to maintain cellular homeostasis and regulate cell fate[49,50], selective targeting of a pathologic methyltransferase complex may exhibit a therapeutic window and not lead to complete ‘shut off’ of an essential epigenetic “writer”. Indeed, we found that SAH-EZH2 arrested the growth and induced differentiation of EZH2-dependent leukemia cells, yet had little demonstrable effect on non-tumorigenic hematopoietic cells. These findings underscore the sequence- and context-dependent anti-proliferative activity of SAH-EZH2.

Online Methods

Synthesis of Stabilized Alpha-Helix of EZH2 Peptides

SAH-EZH2 peptides were designed based on the EED-binding domain of EZH2, with replacement of natural amino acids with olefinic residues at sites on the non-interacting face of the EZH2 helix, as defined by X-ray crystallography[22]. Hydrocarbon stapling, peptide purification to >95% homogeneity, quantitation, and characterization by circular dichroism were performed as previously described in detail [25,52–54]. SAH-EZH2 peptides were synthesized on a 0.05 mmol scale with typical yields exceeding 10 mg per run. The sequence compositions and observed masses of SAH-EZH2 peptides synthesized, purified, and applied in this study are presented in Supplementary Table 2 and Supplementary Fig. 20.

Cell Lines and Tissue Culture

MLL-AF9 leukemia cells were generated as described in Krivtsov et al.[34] and cultured in the MLL-AF9 media, containing IMDM (Invitrogen) and supplemented with 5% fetal calf serum (FCS), 5 ng/ml mouse recombinant IL3 (R&D systems), and 1% penicillin/streptomycin (Invitrogen). COS7 cells (ATCC) were cultured in DMEM media (Invitrogen) supplemented with 10% FCS and 1% penicillin/streptomycin. Sf21 cells (Invitrogen) were cultured in Grace insect media (Invitrogen) supplemented with 10% FCS and 1% penicillin/streptomycin.

SAH-EZH2/EED Binding Analyses

For fluorescence polarization binding analysis, C-terminal His-tagged EED (His-EED) was expressed in *Escherichia coli* BL21(DE3) using 0.3 mM IPTG for 6 h at room temperature. Bacterial pellet lysate was loaded onto a Ni-NTA column (Novagen) for purification of His-EED. Fluorescinated stapled peptides (final concentration, 25 nM) were incubated with His-EED (serial dilution range, 25 nM-8 μM) at room temperature until equilibrium was reached (~15 min). Binding activity was measured by fluorescence polarization on a Perkin-Elmer LS50B luminescence 5 spectrophotometer. K_D values were determined using GraphPad Prism software by following equation,

$$y = AF + \left(\frac{AB - AF}{L}\right) \times \frac{L + KD + X - \sqrt{(L + KD + X)^2 - 4 \times L \times X}}{2}$$

y: Fluorescence polarization, *X*: Receptor concentration, *L*: Ligand concentration

AF: Minimum value of y, *AB*: Maximum value of y

For anti-FITC pull down-based binding assays, HA-EED was produced in Sf21 cells as described previously [19,28]. FITC-SAH-EZH2 peptides (final concentration, 50, 10, and 2 nM) were mixed with 2 μl, 0.5 μl and 0.2 μl of anti-FITC antibody (Abcam, 1 mg/ml) respectively, and incubated with 30 μl of protein G agarose (Roche) in 400 μl binding buffer (pH 8.0, 20 mM Tris-HCl, 150 mM NaCl, 0.3% NP40, 10% glycerol). After successive washes, HA-EED (final concentration of 40 nM each tube) was added and incubated for 3 h, followed by table-top centrifugation and detection of HA-EED bound to FITC-SAH-EZH2 peptides by anti-HA (Santa Cruz Biotechnology) western analysis. Detection of FITC-SAH-EZH2 peptides was accomplished by fluorescence scan (GE Healthcare Life Sciences, Typhoon 9200).

Cellular Uptake of SAH-EZH2 Peptides

MLL-AF9 leukemia cells were seeded in 48-well plates at densities of $2.0X10^5$ cells per well in 200 μl of MLL-AF9 media (5% FCS). FITC-SAH-EZH2 peptides (final concentrations, 4, 2 and 1 μM) were added to the cells and incubated for 8 h. Cells were then washed three times with phosphate buffer saline (PBS, Sigma) and then trypsinized (0.05% Trypsin-EDTA, Invitrogen) at 37°C for 5 min to remove any residual peptide attached to the cell surface. The cells were lysed with SDS loading buffer (Biorad) and brief sonication.

Lysates were electrophoresed on SDS-PAGE gels (Biorad, Criterion tris-tricine 10–20%) and subjected to fluorescence scan (GE healthcare, Typhoon imager 9400).

Confocal Microscopy

COS7 cells were plated in 8-well CC^{2} ™ Chamber Slides ™(Nunc) for 1–2 days prior to experimentation. Slides were washed twice with serum-free DMEM media (Invitrogen) and FITC-SAH-EZH2 peptides were added in DMEM media containing 5% FCS at a final concentration of 5 μM. After 8 h incubation, slides were washed three times with PBS and fixed with 4% paraformaldehyde (Electron Microscopy) for 12 min. After blocking with 5% goat serum (Vector) and staining with EED antibody (Millipore, produced in rabbit), the slides were stained with Alexa Fluor 647 donkey anti-rabbit IgG (Invitrogen). Nuclei were stained upon application of mounting medium containing DAPI (Vector). Confocal images were acquired on a Zeiss LSM700 microscopy and analyzed with ZEN 2011 software (Zeiss).

Immunoprecipitation Analyses

To assess the interaction between SAH-EZH2 peptides and native EED, MLL-AF9 leukemia cells (2×10^{7}) were cultured in 10 ml AF9 media using 10 cm dishes (BD Biosciences) and FITC-SAH-EZH2 peptides added to final concentration of 10 μM, followed by 8–12 h incubation. Treated cells were washed and trypsinized as above, lysed and then incubated with 50 μl of FITC-antibody (1 mg/ml) and 100 μl of protein G agarose (Roche) for 3 h. The amount of EED bound to FITC-SAH-EZH2 peptides was assessed by anti-EED western analysis (Millipore). To monitor for dissociation of native EED-EZH1/EZH2 complexes by SAH-EZH2, Sf21 cells were co-transfected with HA-EED and FLAG-EZH1 or FLAG-EZH2 baculovirus. EED-EZH1 and EED-EZH2 complexes were purified by anti-FLAG agarose (Sigma) (Supplementary Fig. 6). EED-EZH1 and EED-EZH2 complexes (40 nM final concentration) were incubated with FITC-SAH-EZH2 peptides (final concentrations, 10, 3 and 1 μM) in 200 μl binding buffer for 2 h. After successive washes, the mixtures were incubated with anti-HA agarose (Sigma) and the level of HA-EED-bound EZH1 and EZH2 assessed by anti-FLAG western analysis.

Analysis of Trimethylation Status

MLL-AF9 leukemia cells were seeded in 48-well plates at densities of 2×10^{5} cells per well in 200 μl of AF9 media (5% FCS) and then treated with SAH-EZH2 peptides (10 μM) twice daily for 7 days. Cells were then lysed in loading buffer (Biorad) with brief sonication and electrophoresed on SDS-PAGE gels (Thermoscientific, 4–20%). Levels of Lys4 (9751S, cell signaling), Lys9 (5327s, cell signaling), Lys27 (07-449, Millipore) and Lys36 trimethylation (Ab9050, Abcam) were analyzed by the corresponding trimethyl mark-specific antibodies. For flow cytometric analysis of H3 Lys27 trimethylation, MLL-AF9 cells were treated with SAH-EZH2 peptides (10 μM) twice daily for 7 days and then fixed in 70% cold ethanol for overnight at −20 °C. Cells were washed twice in PBS, stained with anti-Lys27-Me3 antibody (Cell Signaling, 9733S) for 20 min and then anti-rabbit IgG Alexafluoro-647 (Invitrogen) for 20 min, followed by FACS analysis using a BD FACSCalibur.

Cell Proliferation, Apoptosis, and Cell Cycle Analyses

To monitor the effect of SAH-EZH2 peptides on cell proliferation, MLL-AF9 cells were seeded in 48 well plates at densities of 2×10^5 cells per well in 150 μl of MLL-AF9 media (5% FCS) and treated with SAH-EZH2 peptides (10 μM) twice daily. Cells were counted every other day using a hematocytometer. To evaluate apoptosis induction, the cells were stained with Annexin V-PE and 7-AAD after 8 or 16 days of treatment with SAH-EZH2 peptides. Camptothecin (Biovision) was used as a positive control (2 μM, 48 h). Cells were analyzed using a BD FACScalibur and data was processed using Flowjo software. For cell cycle analysis, cells were stained with BrdU-APC antibody and 7-AAD (BD Biosciences) after 3 or 6 days of treatment with SAH-EZH2 peptides and 45 min of BrdU incorporation. Cells were analyzed using a BD FACSCalibur.

Cell Viability Assays

For cells with rapid growth, such as MLL-AF9, 32D, MDA-MB231 and DU145, cells were plated at low density (1000/well, 96 well plates), and treated in serum-containing media for the indicated durations with twice daily SAH-EZH2 and single dose GSK126 as reported[21]. Cell viability was measured by CellTiter-Glo (Promega) after 7 days of incubation. For cells with slower growth, such as the B-cell lymphoma lines, cells were plated at higher density (10,000 cells/well for OCI-Ly19, 5,000 cells/well for Karpas422, and 20,000 cells/well for Pfeiffer, 96 well plates) and treated with SAH-EZH2 and GSK126 as above. Cell viability was measured by CellTiter-Glo on days 4, 8 and 12 of treatment by cellular withdrawal and then replacement of equivalent media volumes, with replenishment of GSK126 to maintain treatment concentrations and incubation volumes.

High throughput microfluidic qPCR

Individual primer sets (total of 288) were pooled to a final concentration of 0.1 μM for each primer. One ng of each RNA sample was pre-amplified using pooled primers and CellsDirect RT/Taq enzyme (Invitrogen). Reverse transcription was performed at 50°C for 30 min. Subsequently, in the same tube, cDNA was subjected to sequence-specific amplification by denaturing at 95°C for 15 sec, annealing and amplification at 60°C for 5 min for 14 cycles. Pre-amplified products were diluted 5-fold prior to analysis with Universal PCR Master Mix (Applied Biosystems), EvaGreen Binding Dye (Biotium) and individual qPCR primers in 96×96 Dynamic Arrays on a BioMark System (Fluidigm). Ct values were calculated using the system's software (BioMark Real-Time PCR Analysis; Fluidigm). Ct values of genes were normalized by subtracting Ct values of β-actin, then normalized Ct values subtracted from 28 were used to generate the heatmap.

Cellular Differentiation Analyses

To monitor the morphology of treated cells, MLL-AF9 leukemia cells were exposed to SAH-EZH2 peptides in MLL-AF9 media (5% FCS) for 14 days, as described above. Cells were counted and then diluted into Methocult (STEMCELL technologies) supplemented with 10 ng/ml IL3, 10 ng/ml IL6, 10 ng/ml SCF, 5% FCS, and 1% penicillin/streptomycin at a density of 1000 cells/ml with continued exposure to SAH-EZH2 peptides (10 μM). Aliquots of methocult (1 ml) were plated in 3 cm dishes (BD Biosciences) and colonies

counted after 7 day incubation. Cells were washed with PBS (Sigma), cytospun, and then stained using modified Giemsa stain (Sigma). Morphology was assessed by light microscopy (Nikon Eclipse E800 microscope). HPC5 cells were treated as above except that a higher concentration of SCF (100 ng/ml) was used in the culture media. To detect macrophage-specific cell surface marker expression, MLL-AF9 cells were treated with SAH-EZH2 peptides for 7 d followed by successive washes in PBS and immunostaining with Rat Anti Mouse F4/80 Antigen Alexa 647 (AbD Serotec) and PE Anti-Mouse Neutrophils Monoclonal antibody (CEDARLANE) antibodies. Cells were analyzed by BD FACS Calibur and data processed using Flowjo software.

Statistics

p-values were calculated using 'R' software with the following function:

Sample_A=c(A_1, A_2, A_3);Sample_B=c(B_1,B_2,B_3);t.test(Sample_A, Sample_B)$p. value

A_1, A_2, A_3: Values of sample A

Standard Error of the Mean (s.e.m.) was calculated in accordance with the following equation from Excel software:

s.e.m.=STDEV(a_1,a_2⋯..a_{n-1},a_n)/SQRT(n)

a_1,a_2⋯..a_{n-1},a_n: Values of samples

Supplementary Material

Refer to Web version on PubMed Central for supplementary material.

Acknowledgments

We thank E. Smith for graphics assistance. This work was supported by NIH grant U01CA105423 to S.H.O. and 5R01GM090299 and a Leukemia and Lymphoma Society SCOR project grant to L.D.W. S.H.O. is an Investigator of the Howard Hughes Medical Institute.

References

1. Cao R. Role of Histone H3 Lysine 27 Methylation in Polycomb-Group Silencing. Science. 2002; 298:1039–1043. [PubMed: 12351676]
2. Czermin B, et al. Drosophila enhancer of Zeste/ESC complexes have a histone H3 methyltransferase activity that marks chromosomal Polycomb sites. Cell. 2002; 111:185–196. [PubMed: 12408863]
3. Müller J, et al. Histone methyltransferase activity of a Drosophila Polycomb group repressor complex. Cell. 2002; 111:197–208. [PubMed: 12408864]
4. Kuzmichev A. Histone methyltransferase activity associated with a human multiprotein complex containing the Enhancer of Zeste protein. Genes & Development. 2002; 16:2893–2905. [PubMed: 12435631]
5. Varambally S, et al. The polycomb group protein EZH2 is involved in progression of prostate cancer. Nature. 2002; 419:624–629. [PubMed: 12374981]
6. Kleer CG, et al. EZH2 is a marker of aggressive breast cancer and promotes neoplastic transformation of breast epithelial cells. Proc Natl Acad Sci USA. 2003; 100:11606–11611. [PubMed: 14500907]

7. He LR, et al. High expression of EZH2 is associated with tumor aggressiveness and poor prognosis in patients with esophageal squamous cell carcinoma treated with definitive chemoradiotherapy. Int J Cancer. 2009; 127:138–147. [PubMed: 19904743]
8. Wang C, et al. EZH2 Mediates epigenetic silencing of neuroblastoma suppressor genes CASZ1, CLU, RUNX3, and NGFR. Cancer Research. 2012; 72:315–324. [PubMed: 22068036]
9. Yu J, et al. Integrative Genomics Analysis Reveals Silencing of β-Adrenergic Signaling by Polycomb in Prostate Cancer. Cancer Cell. 2007; 12:419–431. [PubMed: 17996646]
10. Kong D, et al. Loss of let-7 up-regulates EZH2 in prostate cancer consistent with the acquisition of cancer stem cell signatures that are attenuated by BR-DIM. PLoS ONE. 2012; 7:e33729. [PubMed: 22442719]
11. Varambally S, et al. Genomic Loss of microRNA-101 Leads to Overexpression of Histone Methyltransferase EZH2 in Cancer. Science. 2008; 322:1695–1699. [PubMed: 19008416]
12. Morin RD, et al. Somatic mutations altering EZH2 (Tyr641) in follicular and diffuse large B-cell lymphomas of germinal-center origin. Nature Genetics. 2010; 42:181–185. [PubMed: 20081860]
13. McCabe MT, et al. Mutation of A677 in histone methyltransferase EZH2 in human B-cell lymphoma promotes hypertrimethylation of histone H3 on lysine 27 (H3K27). Proceedings of the National Academy of Sciences. 2012; 109:2989–2994.
14. Béguelin W, et al. EZH2 Is Required for Germinal Center Formation and Somatic EZH2 Mutations Promote Lymphoid Transformation. Cancer Cell. 2013; 23:677–692. [PubMed: 23680150]
15. Fussbroich B, et al. EZH2 Depletion Blocks the Proliferation of Colon Cancer Cells. PLoS ONE. 2011; 6:e21651. [PubMed: 21765901]
16. Fujii S, Ito K, Ito Y, Ochiai A. Enhancer of Zeste Homologue 2 (EZH2) Down-regulates RUNX3 by Increasing Histone H3 Methylation. Journal of Biological Chemistry. 2008; 283:17324–17332. [PubMed: 18430739]
17. Wilson BG, et al. Epigenetic Antagonism between Polycomb and SWI/SNF Complexes during Oncogenic Transformation. Cancer Cell. 2010; 18:316–328. [PubMed: 20951942]
18. Chamberlain SJ, Yee D, Magnuson T. Polycomb repressive complex 2 is dispensable for maintenance of embryonic stem cell pluripotency. Stem Cells. 2008; 26:1496–1505. [PubMed: 18403752]
19. Shen X, et al. Jumonji Modulates Polycomb Activity and Self-Renewal versus Differentiation of Stem Cells. Cell. 2009; 139:1303–1314. [PubMed: 20064376]
20. Knutson SK, et al. A selective inhibitor of EZH2 blocks H3K27 methylation and kills mutant lymphoma cells. Nature Chemical Biology. 201210.1038/nchembio.1084
21. McCabe MT, et al. EZH2 inhibition as a therapeutic strategy for lymphoma with EZH2-activating mutations. Nature. 201210.1038/nature11606
22. Han Z, et al. Structural Basis of EZH2 Recognition by EED. Structure. 2007; 15:1306–1315. [PubMed: 17937919]
23. Neff T, et al. Polycomb repressive complex 2 is required for MLL-AF9 leukemia. Proceedings of the National Academy of Sciences. 2012; 109:5028–5033.
24. Shi J, et al. The Polycomb complex PRC2 supports aberrant self-renewal in a mouse model of MLL-AF9;Nras(G12D) acute myeloid leukemia. Oncogene. 201210.1038/onc.2012.110
25. Walensky LD. Activation of Apoptosis in Vivo by a Hydrocarbon-Stapled BH3 Helix. Science. 2004; 305:1466–1470. [PubMed: 15353804]
26. Moellering RE, et al. Direct inhibition of the NOTCH transcription factor complex. Nature. 2009; 462:182–188. [PubMed: 19907488]
27. Deshayes S, Morris MC, Divita G, Heitz F. Cell-penetrating peptides: tools for intracellular delivery of therapeutics. Cell Mol Life Sci. 2005; 62:1839–1849. [PubMed: 15968462]
28. Shen X, et al. EZH1 Mediates Methylation on Histone H3 Lysine 27 and Complements EZH2 in Maintaining Stem Cell Identity and Executing Pluripotency. Molecular Cell. 2008; 32:491–502. [PubMed: 19026780]
29. Ezhkova E, et al. EZH1 and EZH2 cogovern histone H3K27 trimethylation and are essential for hair follicle homeostasis and wound repair. Genes & Development. 2011; 25:485–498. [PubMed: 21317239]

30. Margueron R, et al. Ezh1 and Ezh2 Maintain Repressive Chromatin through Different Mechanisms. Molecular Cell. 2008; 32:503–518. [PubMed: 19026781]
31. Byvoet P, Shepherd GR, Hardin JM, Noland BJ. histone half-life. Archives of Biochemistry and Biophysics. 2003; 148:558–567. [PubMed: 5063076]
32. Sasaki M, Yamaguchi J, Itatsu K, Ikeda H, Nakanuma Y. Over-expression of polycomb group protein EZH2 relates to decreased expression of p16 INK4a in cholangiocarcinogenesis in hepatolithiasis. J Pathol. 2008; 215:175–183. [PubMed: 18393368]
33. Bracken AP, et al. The Polycomb group proteins bind throughout the INK4A-ARF locus and are disassociated in senescent cells. Genes & Development. 2007; 21:525–530. [PubMed: 17344414]
34. Krivtsov AV, et al. Transformation from committed progenitor to leukaemia stem cell initiated by MLL–AF9. Nature. 2006; 442:818–822. [PubMed: 16862118]
35. Toren A, et al. CD133-positive hematopoietic stem cell 'stemness' genes contain many genes mutated or abnormally expressed in leukemia. Stem Cells. 2005; 23:1142–1153. [PubMed: 16140871]
36. Suetsugu A, et al. Characterization of CD133+ hepatocellular carcinoma cells as cancer stem/progenitor cells. Biochemical and Biophysical Research Communications. 2006; 351:820–824. [PubMed: 17097610]
37. Singh SK, et al. Identification of human brain tumour initiating cells. Nature. 2004; 432:396–401. [PubMed: 15549107]
38. Di Tullio A, Vu Manh TP, Schubert A, Månsson R, Graf T. CCAAT/enhancer binding protein alpha (C/EBP(alpha))-induced transdifferentiation of pre-B cells into macrophages involves no overt retrodifferentiation. Proceedings of the National Academy of Sciences. 2011; 108:17016–17021.
39. Pinto do OP. Hematopoietic progenitor/stem cells immortalized by Lhx2 generate functional hematopoietic cells in vivo. Blood. 2002; 99:3939–3946. [PubMed: 12010792]
40. Lee ST, et al. Context-specific regulation of NF-κB target gene expression by EZH2 in breast cancers. Molecular Cell. 2011; 43:798–810. [PubMed: 21884980]
41. Xu K, et al. EZH2 oncogenic activity in castration-resistant prostate cancer cells is Polycomb-independent. Science. 2012; 338:1465–1469. [PubMed: 23239736]
42. You JS, Jones PA. Cancer genetics and epigenetics: two sides of the same coin? Cancer Cell. 2012; 22:9–20. [PubMed: 22789535]
43. Hinz S, et al. Expression of the polycomb group protein EZH2 and its relation to outcome in patients with urothelial carcinoma of the bladder. J Cancer Res Clin Oncol. 2007; 134:331–336. [PubMed: 17694325]
44. Tan J, et al. Pharmacologic disruption of Polycomb-repressive complex 2-mediated gene repression selectively induces apoptosis in cancer cells. Genes & Development. 2007; 21:1050–1063. [PubMed: 17437993]
45. Momparler RL, Idaghdour Y, Marquez VE, Momparler LF. Synergistic antileukemic action of a combination of inhibitors of DNA methylation and histone methylation. Leuk Res. 2012; 36:1049–1054. [PubMed: 22472464]
46. Miranda TB, et al. DZNep is a global histone methylation inhibitor that reactivates developmental genes not silenced by DNA methylation. Molecular Cancer Therapeutics. 2009; 8:1579–1588. [PubMed: 19509260]
47. Chiang PK. Biological effects of inhibitors of S-adenosylhomocysteine hydrolase. Pharmacol Ther. 1998; 77:115–134. [PubMed: 9578320]
48. Borchardt RT, Keller BT, Patel-Thombre U. Neplanocin A. A potent inhibitor of S-adenosylhomocysteine hydrolase and of vaccinia virus multiplication in mouse L929 cells. J Biol Chem. 1984; 259:4353–4358. [PubMed: 6707008]
49. Bowen NJ, Fujita N, Kajita M, Wade PA. Mi-2/NuRD: multiple complexes for many purposes. Biochim Biophys Acta. 2004; 1677:52–57. [PubMed: 15020045]
50. Ho L, Crabtree GR. Chromatin remodelling during development. Nature. 2010; 463:474–484. [PubMed: 20110991]
51. Chou TC. Theoretical basis, experimental design, and computerized simulation of synergism and antagonism in drug combination studies. Pharmacol Rev. 2006; 58:621–681. [PubMed: 16968952]

52. Walensky LD, et al. A Stapled BID BH3 Helix Directly Binds and Activates BAX. Molecular Cell. 2006; 24:199–210. [PubMed: 17052454]

53. Stewart ML, Fire E, Keating AE, Walensky LD. The MCL-1 BH3 helix is an exclusive MCL-1 inhibitor and apoptosis sensitizer. Nature Chemical Biology. 2010; 6:595–601. [PubMed: 20562877]

54. Bird GH, et al. Hydrocarbon double-stapling remedies the proteolytic instability of a lengthy peptide therapeutic. Proceedings of the National Academy of Sciences. 2010; 107:14093–14098.

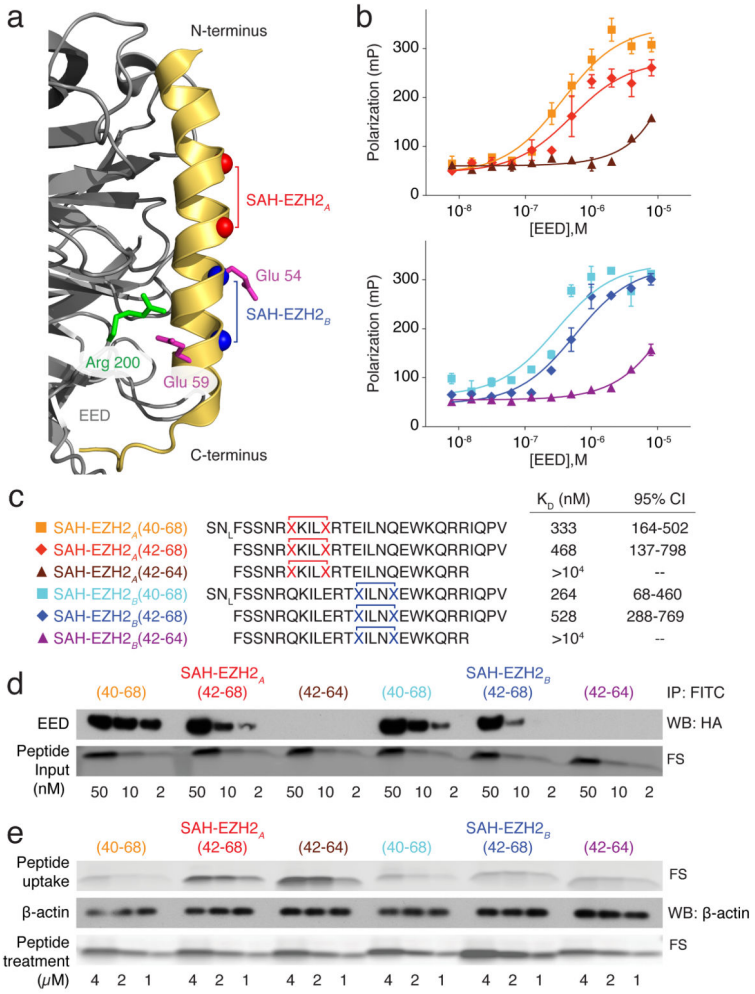

Figure 1. Synthesis, EED-binding activity, and cellular penetration of SAH-EZH2 peptides

a) Design of hydrocarbon-stapled peptides to recapitulate the bioactive structure of the EED-binding domain of EZH2. The location of stapling position 'A' (47–51) is marked with red spheres and position 'B' (54–58) is marked with blue spheres. The alpha-helical EED-binding domain of EZH2 is colored gold and EED is colored gray. The native methionine of SAH-EZH2 was replaced with norleucine ('N_L') due to the incompatibility of sulfur with the metathesis reaction.

b) Binding affinity of SAH-EZH2 peptides for EED as measured by fluorescence polarization assay. Data represents mean ± s.e.m. for experiments performed in triplicate.

c) Sequences and binding affinities of SAH-EZH2 peptides. CI, confidence interval

d) Anti-FITC immunoprecipitation of purified HA-EED (40 nM) upon incubation with the indicated amounts of FITC-labeled SAH-EZH2 peptides. The results are representative of experiments performed in duplicate. FS, Fluorescence Scan. Full gel image in Supplementary Fig. 21

e) Cellular penetration of SAH-EZH2 peptides. Lysates of treated MLL-AF9 leukemia cells were electrophoresed and analyzed by fluorescence scan. The results are representative of

experiments performed in duplicate. FS, Fluorescence Scan. Full gel image in Supplementary Fig. 21

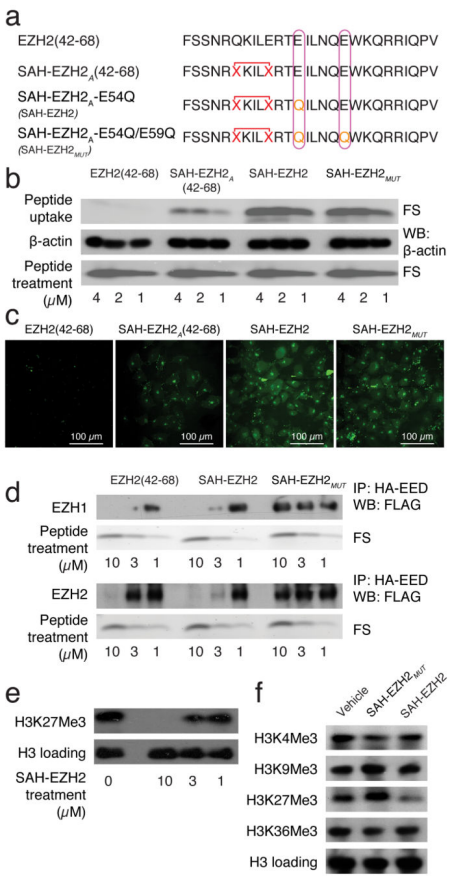

Figure 2. Sequence-dependent dissociation of EED-EZH1/EZH2 complexes and impairment of PRC2 activity by SAH-EZH2

a) Sequences of SAH-EZH2 and its mutants

b) Enhanced cellular penetration of the E54Q (SAH-EZH2) and E54Q/E59Q (SAH-EZH2$_{MUT}$) mutants of SAH-EZH2$_A$(42-68), as measured by fluorescence scan of lysates from FITC-peptide treated MLL-AF9 leukemia cells at 8 hours. The results are representative of experiments performed in duplicate. FS, Fluorescence Scan. Full gel image in Supplementary Fig. 21

c) Comparative cellular uptake of EZH2, SAH-EZH2$_A$(42-68), SAH-EZH2, and SAH-EZH2$_{MUT}$ peptides, as measured by confocal microscopy of FITC-peptide treated (5 μM) COS-7 cells at 8 hours. The results are representative of experiments performed in triplicate.

d) Dissociation of HA-EED/EZH1 and HA-EED/EZH2 complexes (40 nM) by SAH-EZH2, but not SAH-EZH2$_{MUT}$, peptides at the indicated doses, as assessed by anti-HA pull-down and EZH1/EZH2 western analysis. FS, Fluorescence Scan. Full gel image in Supplementary Fig. 21

e) Dose-responsive suppression of H3K27 trimethylation by SAH-EZH2, administered to cultured MLL-AF9 cells twice daily for 7 days at 1, 3, and 10 μM dosing. Full gel image in Supplementary Fig. 21

f) Selective reduction of H3K27Me3 by SAH-EZH2, as assessed by trimethylation mark western analysis. MLL-AF9 leukemia cells were treated with SAH-EZH2 or SAH-EZH2$_{MUT}$ (10 μM) twice daily for 7 days prior to analysis.

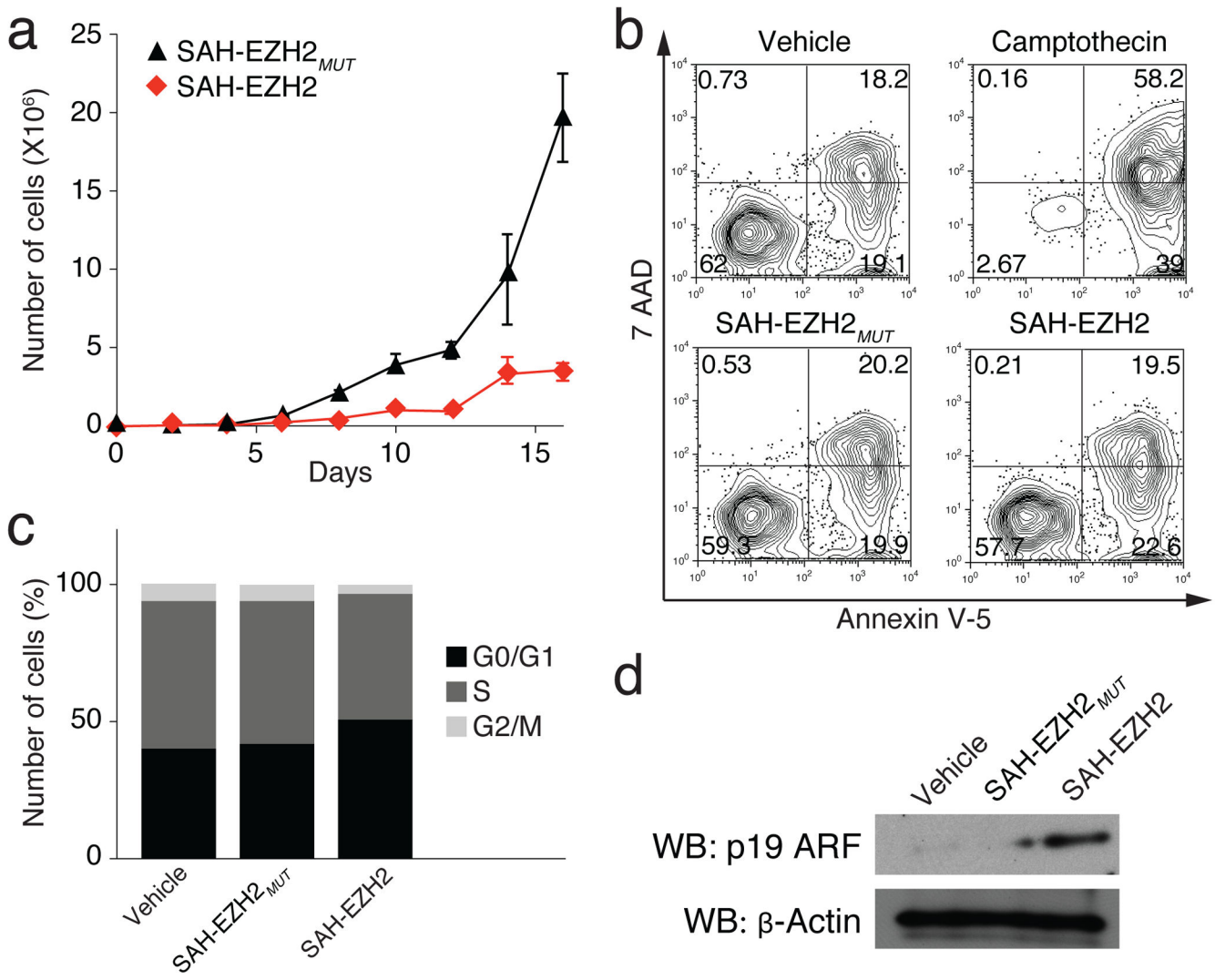

Figure 3. SAH-EZH2 induces cell cycle arrest and inhibits proliferation of MLL-AF9 leukemia cells

a) SAH-EZH2 (10 μM, twice daily), but not its mutant control, inhibits the proliferation of MLL-AF9 cells. Data represent mean ± s.e.m for independent experiments performed in triplicate.

b) The anti-leukemic activity of SAH-EZH2 is not mediated by a pro-apoptotic effect, as evidenced by FACS analysis and Annexin V/7-AAD staining after 8 days of treatment with SAH-EZH2 peptides (10 μM, twice daily).

c) Cell cycle analysis of SAH-EZH2-treated (10 μM, twice daily) cells. Cells were stained with BrdU-APC antibody and 7-AAD and analyzed by flow cytometry after 6 days of treatment. Data represent mean ± s.e.m for independent experiments performed in duplicate (see also Supplementary Table1).

d) SAH-EZH2, but not its mutant control, upregulates the expression of p19ARF upon treatment of MLL-AF9 cells for 7 days (10 μM, twice daily), as assessed by western analysis. Full gel image in Supplementary Fig. 21

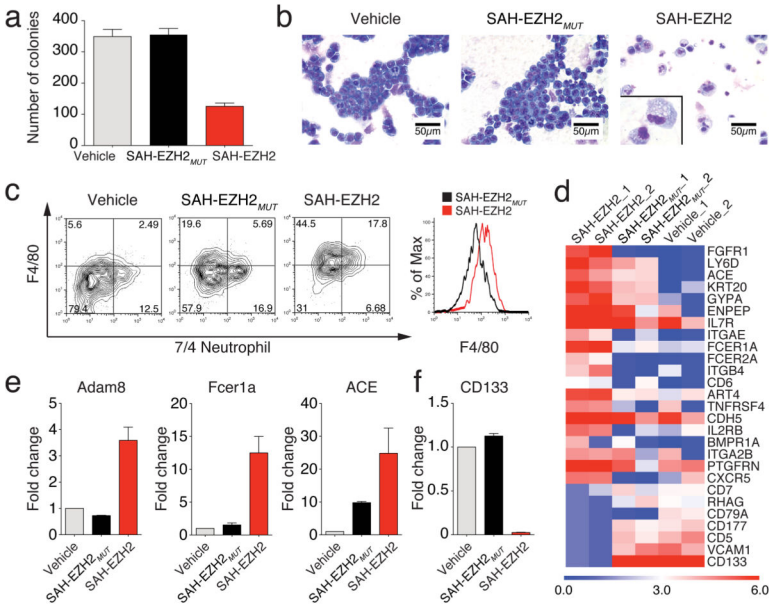

Figure 4. SAH-EZH2 induces monocyte/macrophage differentiation of MLL-AF9 leukemia cells

a) Suppression of colony-forming potential by SAH-EZH2 as compared to vehicle (water) and SAH-EZH2$_{MUT}$, p<0.02. MLL-AF9 cells were treated as described in Methods. Data represent mean and s.e.m for independent experiments performed in duplicate.

b) Morphology of SAH-EZH2-treated MLL-AF9 leukemia cells. Whereas vehicle and SAH-EZH2$_{MUT}$ -treated cells retain characteristic blastic features, SAH-EZH2-treated cells exhibit the morphology of monocyte/macrophage differentiation.

c) Flow cytometric analysis of macrophage-specific cell surface marker expression (F4/80) of SAH-EZH2-treated MLL-AF9 cells at 8 days (10 μM, twice daily).

d) Comparative changes in cell surface marker gene expression in MLL-AF9 cells treated with vehicle (water), SAH-EZH2, or SAH-EZH2$_{MUT}$ for 8 days (10 μM, twice daily). CT-value was processed as described in Methods and the transcripts that increased/decreased by more than 6 fold were plotted.

e) Real Time qPCR analysis of macrophage/monocyte-specific marker expression. SAH-EZH2-treated (10 μM, twice daily for 8 days) cells exhibit increased expression of macrophage/monocyte specific markers. Data represent mean and s.e.m for independent experiments performed in duplicate. p_{Adam8}<0.11, p_{Fcer1a}<0.14, p_{ACE}< 0.29. p values were calculated based on data comparison between SAH-EZH2 and SAH-EZH2$_{MUT}$ treatments.

f) Decreased CD133 expression in SAH-EZH2-treated (10 μM, twice daily for 8 days) MLL-AF9 leukemia cells, p_{CD133}<0.015. p values were calculated based on data comparison between SAH-EZH2 and SAH-EZH2$_{MUT}$ treatments.

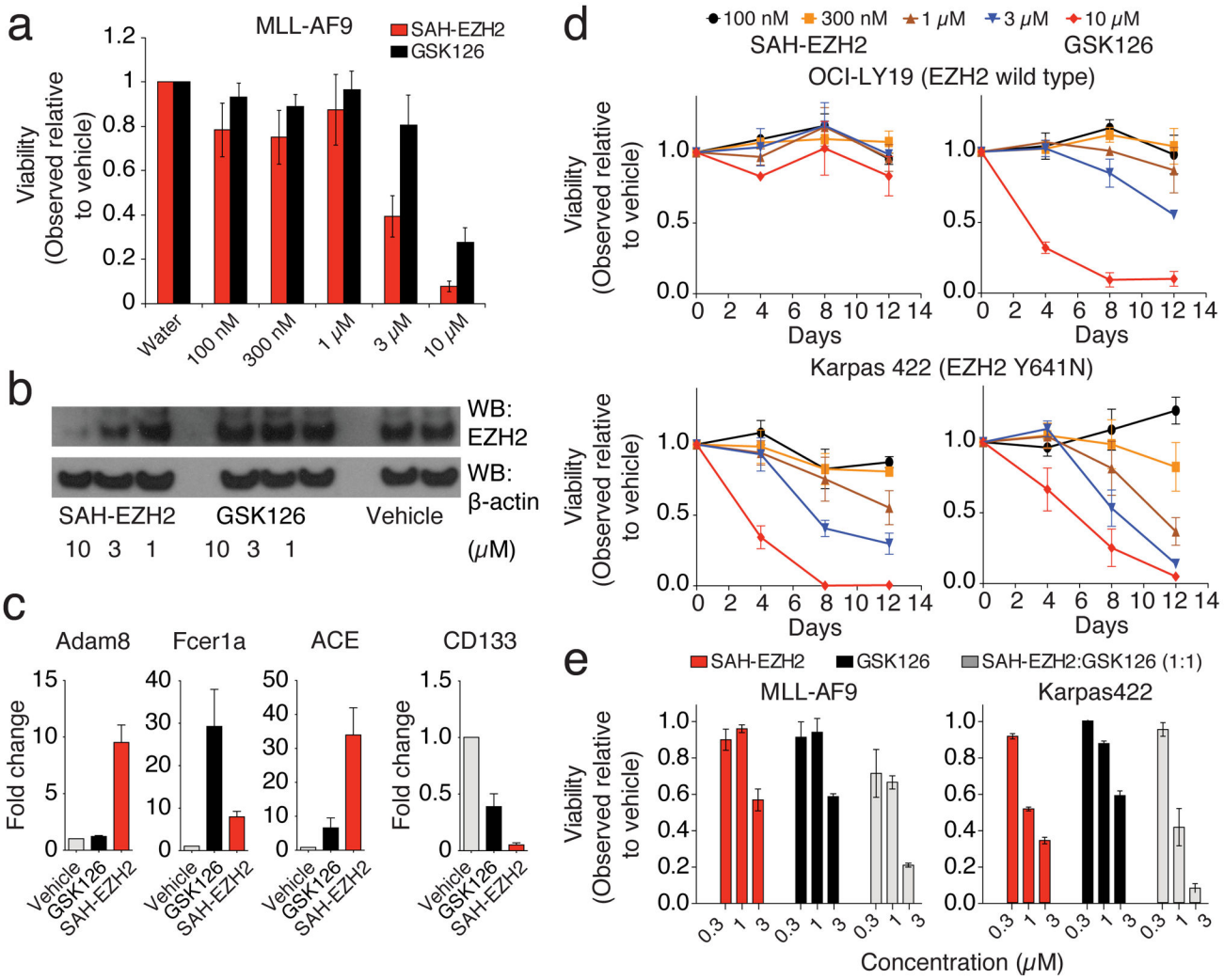

Figure 5. Cell Viability Effects of SAH-EZH2 and GSK126

a) Dose-responsive effects of SAH-EZH2 and GSK126 treatment on MLL-AF9 leukemia cell viability. Data represent mean ± s.e.m. for experiments performed in biological triplicates and technical duplicates. Cells were treated with SAH-EZH2 (twice daily) and GSK126 (single dose, as reported[21]) in serum-containing media for 7 days.

b) Effects of vehicle (water), SAH-EZH2, and GSK126 treatments on EZH2 protein level in MLL-AF9 cells. Cells were treated with SAH-EZH2 (twice daily) and GSK126 (single dose, and replenished at cell split due to confluency, as reported[21]) for 7 days. Full gel image in Supplementary Fig. 21

c) Cell surface marker expression of MLL-AF9 cells treated with SAH-EZH2 and GSK126 as above for 8 days. Data represent mean ± s.e.m for independent experiments performed in biological and technical duplicates.

d) Dose-responsive effects of SAH-EZH2 and GSK126 treatment on EZH2 wild-type (OCI-LY19) and EZH2 mutant (Karpas422) B-cell lymphoma cell lines. Cells were treated with SAH-EZH2 twice daily and GSK126 at the indicated doses for 12 days. Cells were split at days 4, 8 and 12 for viability measurement and compounds were replenished with fresh

media to maintain concentration. Data represent mean ± s.e.m for experiments performed in biological triplicate and technical duplicate.

e) Effect of combination treatment at the indicated doses with SAH-EZH2 and GSK126 in MLL-AF9 and Karpas422 cells. Calcusyn analysis[51] revealed ED_{50} combination indices (CI) of 0.11 and 0.74 for MLL-AF9 and Karpas422 cells, respectively (CI<1 indicates synergy). Cells were treated twice daily with SAH-EZH2 and single dose GSK126 (as reported[21]) at the indicated concentrations for 7 days. Data represent mean ± s.e.m for experiments performed in biological triplicate.